

# An oxygen isotope data set for marine waters

Grant R. Bigg

School of Environmental Sciences, University of East Anglia, Norwich, England

Eelco J. Rohling

School of Ocean and Earth Sciences, University of Southampton, Southampton Oceanography Centre, Southampton England

**Abstract.** The proportion of  $^{18}\text{O}$  in a sample of seawater is an excellent tracer of its past history as, away from the surface, it is conservative and also nondynamical. The range of values in source waters is also large, and the accuracy achievable in modern measurement high. Here we bring together for the first time a global data set of over 6000 individual measurements from the past 40 years. The properties of this data set are described. Noteworthy features include the hitherto unnoticed, but distinctive, contribution of North Pacific Upper Water to the  $\delta^{18}\text{O}$ :salinity relationship, and different origins of the deeper waters of the Atlantic and Pacific Oceans. We also make a plea here to the international community to contribute unpublished data to the archive for the use of all.

## 1. Introduction

Since the pioneering work of *Epstein and Mayeda* [1953] and *Craig and Gordon* [1965] (henceforth known as CG), it has been known that the proportion of  $\text{H}_2\text{O}^{18}$  in seawater is a very good tracer of water mass origin. In standard mean ocean water (SMOW) the atomic ratio of  $^{18}\text{O}/^{16}\text{O}$  is  $(2005.20 \pm 0.45) \times 10^{-6}$  [Baertschi, 1976], but, measured in terms of

$$\delta^{18}\text{O} = 1000 \frac{(^{18}\text{O}/^{16}\text{O})_{\text{sample}} - (^{18}\text{O}/^{16}\text{O})_{\text{SMOW}}}{(^{18}\text{O}/^{16}\text{O})_{\text{SMOW}}}, \quad (1)$$

$\delta^{18}\text{O}$  can vary from below -20‰ in the runoff from polar landmasses to over 2‰ in highly evaporative, semienclosed basins such as the Red Sea. Modern stable isotope mass spectrometry is such that  $\delta^{18}\text{O}$  can be measured to an accuracy, and precision, of 0.03‰ [Frew *et al.*, 1995], giving it a similar range and accuracy to that other well-used conservative tracer, salinity. Salinity and  $\delta^{18}\text{O}$  are related through both being altered in surface waters by evaporation (CG). However,  $\delta^{18}\text{O}$  has some advantages over salinity in that it is a tracer following the water itself and is not dynamically active. Thus while there are strong relationships between salinity and  $\delta^{18}\text{O}$ , these vary regionally [CG; Ferronsky and Brezgunov, 1982], seasonally [Fairbanks, 1982; Strain and Tan, 1993], and probably on longer timescales [Rohling and Bigg, 1998]. Another way in which  $\delta^{18}\text{O}$  differs significantly from salinity is that inputs of freshwater to the ocean always have the same salinity of nearly 0 psu but widely differing values of  $\delta^{18}\text{O}$ , whether due to precipitation [Dansgaard, 1964], river inflow [Mook, 1982], or glacier calving (CG). Even melting sea ice shows differing character. Its salinity may vary from 5 to 15 psu [Pickard and Emery, 1982], depending on the rapidity of initial freezing, but its  $\delta^{18}\text{O}$  value will be essentially unchanged

from that of the water from which it froze [Tan and Strain, 1980]. Thus both freezing sea ice and the brine rejected from it will have a flat salinity- $\delta^{18}\text{O}$  relationship because of this essential  $\delta^{18}\text{O}$  invariance under freezing.

The relative difficulty of measuring  $\delta^{18}\text{O}$ , and its seeming similarity to salinity has, however, meant that far fewer  $\delta^{18}\text{O}$  measurements are available for the ocean. These have been scattered amongst dozens of sources, some unpublished, since the original analyses of *Epstein and Mayeda* [1953]. There has not yet been a major effort to bring all the data together. The strong mixing of fresh and ocean waters in the coastal environment has long been recognized as a place where oxygen isotopic measurements can clearly delineate water mass formation processes [Fairbanks, 1982]. Only more recently has it been realized that, in addition to providing additional information, the sensitivity of  $\delta^{18}\text{O}$  can be greater than that of salinity in the deep ocean [Frew *et al.*, 1995]. We have therefore attempted to gather together as much marine oxygen isotopic data as possible to provide a data set of potentially wide use within the oceanographic community. Such a data set can also provide much needed oceanic boundary conditions for the increasing employment of  $\text{H}_2\text{O}^{18}$  as a tracer within atmospheric circulation models of the present day [Joussaume *et al.*, 1984; Jouzel *et al.*, 1987; Hoffmann and Heimann, 1993] and for understanding the link between precipitation and oxygen isotopes during glacial periods [Joussaume and Jouzel, 1993; Hoffmann and Heimann, 1997]. Ocean models are also beginning to use this tracer to investigate the influence of advection on the salinity- $\delta^{18}\text{O}$  relationship [Schmidt, 1998] and will require both validation and initialization.

In the following section we will describe the sources, strengths, and limitations of the data set. We then show some standard oceanic profiles to illustrate the robustness of the data and the presence of major features one would expect to find, such as the North Atlantic Deep Water signal. The data set has hidden riches, however, and so we next explore one of these, namely evidence for shallow convection at the subtropical-polar boundary in the Northwest Pacific.

Copyright 2000 by the American Geophysical Union.

Paper number 2000JC900005.  
0148-0227/00/2000JC900005\$09.00

**Table 1.** Sources of Marine  $\delta^{18}\text{O}$  Database

Source			
No.	Reference	No. points	Comments
1	<i>Weiss et al.</i> [1979]	28	Weddell Sea; summer 1973; full depth
2	<i>Epstein and Mayeda</i> [1953]	82	Global; unknown dates; full depth <sup>a</sup>
3	<i>Bedard et al.</i> [1981]	8	Baffin Bay; unknown year; near surface
4	<i>Van Donk and Mathieu</i> [1969]	11	Arctic; unknown month; full depth
5	<i>Tan and Strain</i> [1980]	19	Baffin Bay; summer 1977; full depth
6	<i>Östlund and Hut</i> [1984]	25	Arctic; summer 1981; full depth
7	<i>Duplessey et al.</i> [1981]	9	Indian; summer 1976; surface
8	<i>Merlivat et al.</i> [1987]	1	Pacific; unknown date; deep ocean
9	<i>Moore et al.</i> [1983]	4	Arctic; spring 1979; near surface
10	<i>Vetshteyn et al.</i> [1976]	33	Arctic; winter; full depth
11	<i>Frohlich et al.</i> [1988]	36	Baltic; summer 1983; full depth
12	<i>Andrie and Merlivat</i> [1989]	78	North Atlantic; unknown date; full depth
13	<i>Kippshut</i> [1990]	19	North Pacific; autumn 1982; full depth
14	<i>Pierre et al.</i> [1991]	68	South Atlantic; summer 1987; full depth
15	<i>Swart</i> [1991]	18	Black Sea; summer 1988; upper ocean
16	<i>Létolle et al.</i> [1993]	19	Arctic; autumn 1989; near surface
17	<i>MacDonald et al.</i> [1995]	3	Arctic; through 1991; surface
18	<i>Stenni et al.</i> [1995]	419	Mediterranean; spring 1988; full depth
19	<i>Bauch et al.</i> [1995]	489	Arctic; summer 1987 and 1991; mostly upper ocean but occasional deep profiles
20	<i>Östlund et al.</i> [1987a]	40	Arctic; spring, several years; full depth
21	<i>Gat et al.</i> [1996]	111	Mediterranean; various times; full depth
22	<i>Khim and Krantz</i> [1996]	2	North Atlantic; averages; surface
23	<i>Tan and Strain</i> [1996]	39	Hudson Bay; summer 1982; surface
24	<i>Grebmeier et al.</i> [1990]	70	Arctic; summer 1987/1988; mostly upper ocean
25	<i>Weppernig et al.</i> [1996]	340	Weddell Sea; autumn 1992; full depth
26	<i>Östlund et al.</i> [1987b]	724	Global (GEOSECS); various times; full depth
27	<i>Azetsu-Scott and Tan</i> [1997]	36	North Atlantic; autumn 1993; upper ocean
28	<i>Archambeau et al.</i> [1998]	224	South Atlantic; unknown time; full depth
29	<i>Pierre</i> [1999]	304	Mediterranean; various times; full depth
30	<i>Craig and Gordon</i> [1965]	95	Global; unknown time; full depth, interpolated from figures
31	<i>Heywood et al.</i> [1998]; <i>Frew et al.</i> [2000]; <i>Meredith et al.</i> [1999a]	1161	Atlantic and Indian; various times; full depth
32	<i>Cooper et al.</i> [1997]	1314	Arctic and North Pacific; various times; full depth
33	<i>Pierre et al.</i> [1994]	93	North Atlantic; winter 1991; full depth
34	<i>Wellington et al.</i> [1996]	27	South Pacific; various times; surface
35	<i>Meredith et al.</i> [1999b]	197	South Atlantic; spring 1994; full depth
36	<i>Grossman</i> [1984]	18	North Pacific; unknown times; full depth
37	<i>Mook</i> [1982]	210	Global; various times; surface

<sup>a</sup>The conversion of *Epstein and Mayeda's* [1953]  $\delta$  to SMOW is  $\delta^{18}\text{O}=1.035(\delta+0.2)+0.13$ .

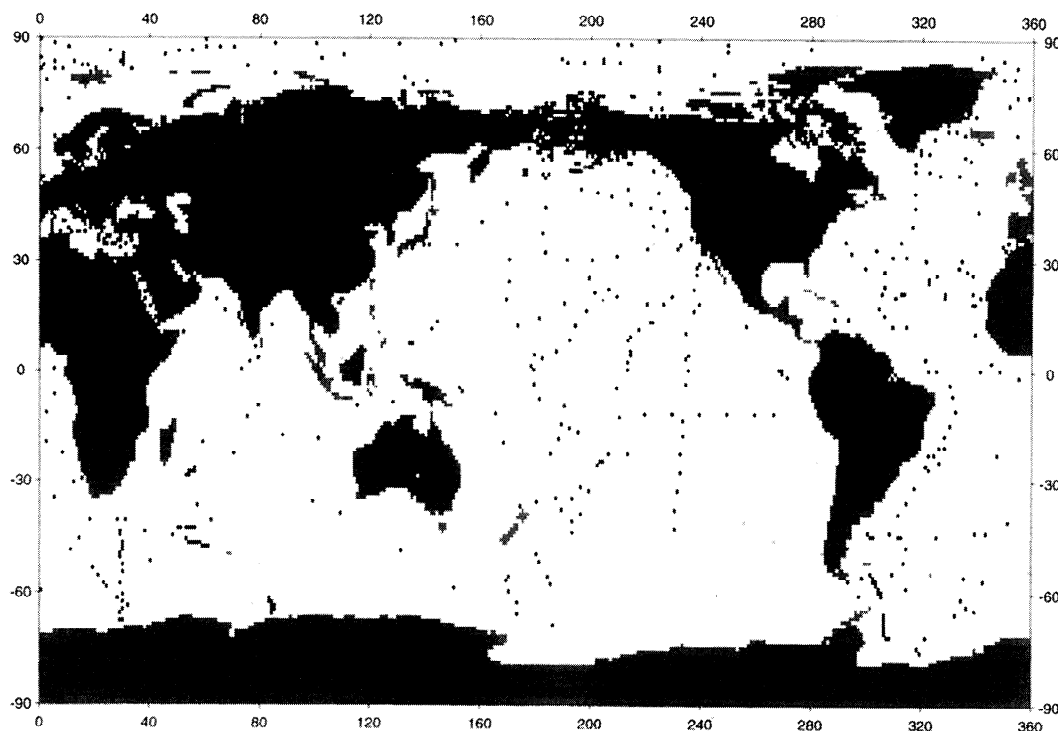


**Figure 1.** Geographical distribution of oxygen isotope data. Each dot represents at least one data point within the  $1^\circ$  latitude  $\times$   $1^\circ$  longitude polygon.

## 2. Compilation of the Data Set, and Geographical Properties

The marine  $\delta^{18}\text{O}$  database currently consists of 6474 separate observations from 37 different sources (Table 1). These cover almost 50 years of sampling, spanning the whole of the global ocean from the central Arctic to the Weddell Sea and from the surface to the deep ocean trenches. Nevertheless, both the spatial and temporal coverage is far from complete. In addition, the precision of data has varied over time, and not all of the data was available in tabular or digital form, nor was it always precisely geographically or temporally located. Where data were interpolated from graphs (see Table 1) the accuracy is  $\pm 0.1\text{‰}$  and the horizontal position is normally known to within  $1^\circ$  of latitude or longitude. In the vertical the 33 standard depths of the Levitus hydrographic climatology [Levitus *et al.*, 1994] have been used for later analysis. Any vertical interpolation required from graphs was accurate enough not to lead to an incorrect standard level being assigned to the data point in this later analysis. If the month and year of observation is not known, then a midsummer month (hemispheric dependent) is attached to the data point, in a year just prior to that of publication of the source. Such data points were flagged, as their use in studies of temporal variation will be suspect. Occasional anomalies were found: where these were not clearly typographical errors, or could not be checked with the original author, the data were excluded from the database. More details about the individual sources can be found in Table 1.

The geographical distribution of the data points is shown in Figure 1. While certain regions, such as the Mediterranean and the Arctic, are quite well covered, there are large data sparse areas in the South Pacific, the Indian Ocean, and the western Pacific. Even the surface Atlantic is rather poorly sampled, although its deeper coverage is better. Figure 2 shows the sample density with

depth. The surface waters are by far the best sampled, with approximately 850 values globally, but most levels have in excess of 100 samples, except for the levels in the depth range 1100–1400 m and deeper than 5000 m. Temporally, the great majority of data have been taken in the summer or autumn (Table 1). Therefore a full seasonal cycle can only be reliably constructed in the Adriatic [Stenni *et al.*, 1995] and the Bering Strait [Cooper *et al.*, 1997] and at a few river outflows [Mook, 1982].

The link between salinity and  $\delta^{18}\text{O}$  is strong because both are affected, in surface waters away from the influence of melting and freezing, by precipitation and evaporation. However, CG showed that there is a large geographical variation in this relationship, with a much weaker slope between the two variables in the equatorial and polar regions than in midlatitudes, for different reasons. Rohling and Bigg [1998] have argued that the form of this relationship, and its zonation, may change over the glacial cycle, if not shorter timescales. A scatterplot of the appropriate seasonal Levitus *et al.*, [1994] salinity versus  $\delta^{18}\text{O}$  for the global data set is shown in Figure 3a. Regions with salinities outside the normal oceanic range [32.0, 40.0] have been excluded, to remove clear riverine influence. The classical extratropical mixing line shown by CG, and reproduced in the modeling work of Schmidt [1998], is seen in the middle of Figure 3. Equatorial surface points also tend to lie along a line with weak slope just above 0‰, as shown by CG.

However, a number of other patterns are also evident. There is a break in the slope of the mixing line near 36.5 psu. At higher salinities the slope is less steep: this is because of mixing between intermediate waters of Mediterranean origin (salinity  $\sim$  39.0 psu,  $\delta^{18}\text{O} \sim 1.5\text{‰}$ ) and Mode Water from the subtropical North Atlantic (salinity  $\sim$  36.0–36.5 psu,  $\delta^{18}\text{O} \sim 1.0\text{‰}$ ). Careful inspection of Figure 3a shows a similar, but much less data rich, offset in the Indian Ocean (relevant points marked by  $\emptyset$ ). Here

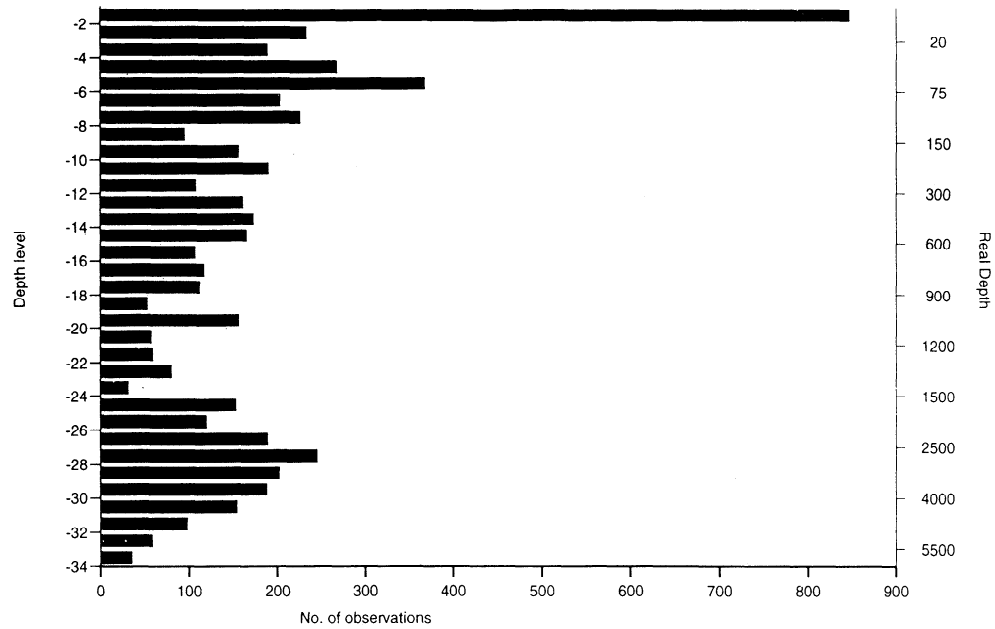


Figure 2. Histogram of number of data points in each level [see Levitus *et al.*, 1994].

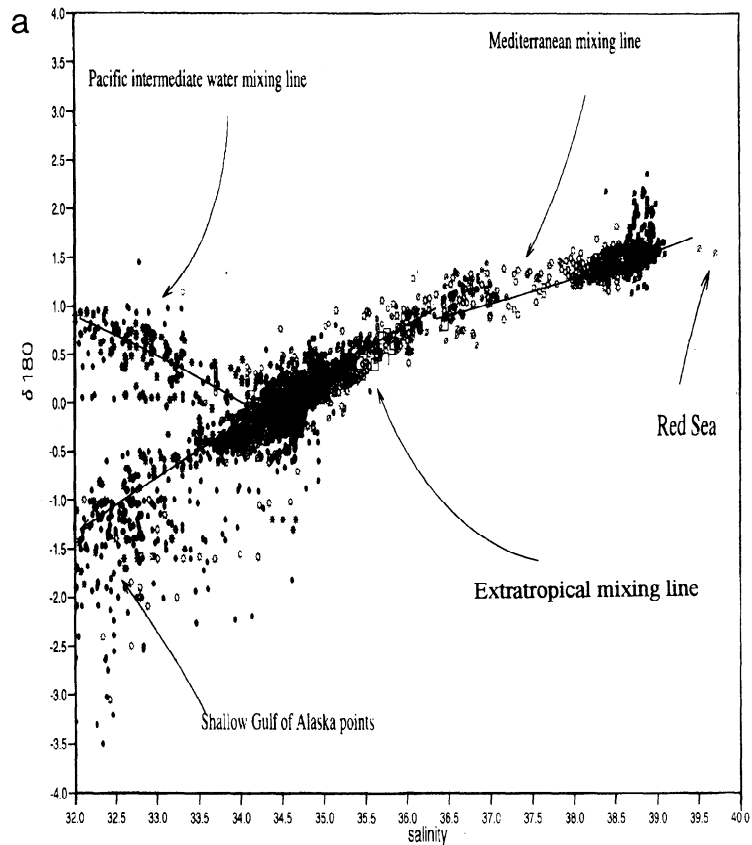


Figure 3. Scatterplot of data points with a salinity  $S > 32.0$  psu and  $\delta^{18}\text{O} > -4\text{‰}$ . The salinity used is always that from Levitus *et al.*, [1994] for consistency. The CG extratropical mixing line, with a slope of  $d\delta^{18}\text{O}/dS=0.60$ , is clearly distinguishable near  $S=34.5$  psu. The data points are coded as open circle, equatorial ( $\pm 10^\circ$ ); solid circle, polar ( $> \pm 65^\circ$ ); circle with four points: North Atlantic ( $80^\circ\text{W}-20^\circ\text{E}$ ); asterisk, North Pacific ( $110^\circ\text{E}-90^\circ\text{W}$ ); circle with cross, South Atlantic ( $70^\circ\text{W}-20^\circ\text{E}$ ); square, South Pacific ( $150^\circ\text{W}-70^\circ\text{W}$ ); null symbol, Indian Ocean ( $20^\circ\text{E}-120^\circ\text{E}$ ,  $60^\circ\text{S}-30^\circ\text{N}$ , excluding equatorial strip); solid circle with bar, Mediterranean ( $0^\circ-40^\circ\text{E}$ ,  $30^\circ-45^\circ\text{N}$ ). Points falling within the equatorial and polar categories are not included in the remaining regions. (a) All data and (b) data from deeper than 1000 m. Note the discontinuity in the mixing line around 34.8 psu in Figure 3b: higher salinity points lie on a Mediterranean-Mode Water mixing line, and lower salinity points involve mixing with Antarctic Intermediate Water.

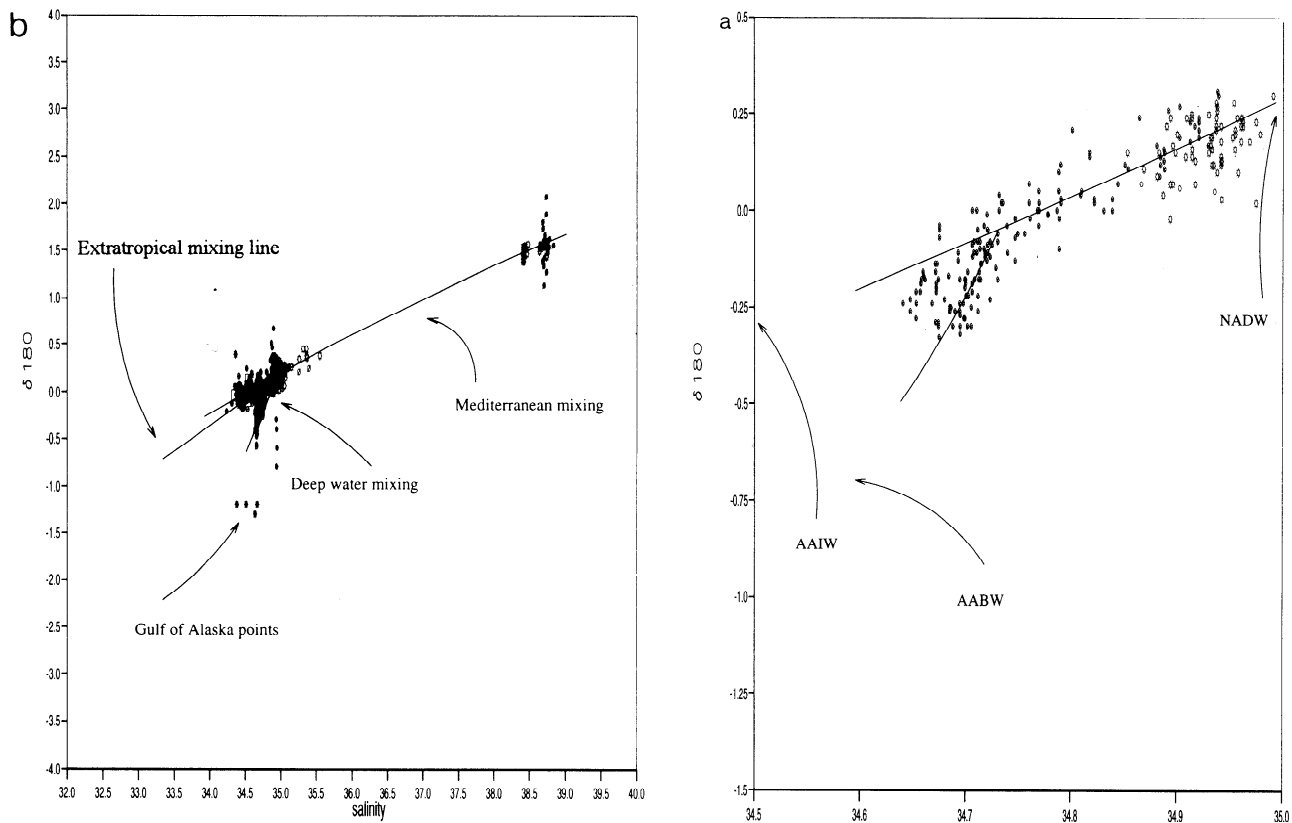


Figure 3. (continued)

there is a high salinity, high  $\delta^{18}\text{O}$  source of intermediate water in the Red Sea (salinity  $\sim 39.5$  psu,  $\delta^{18}\text{O} \sim 1.5\text{‰}$ ) mixing with Intermediate Water deriving from the Southern Indian Ocean (salinity  $\sim 36.5$  psu,  $\delta^{18}\text{O} \sim 0.8\text{‰}$ ).

The slope discontinuity is supported when viewing only data from 1050 m or deeper (Figure 3b). This latter figure shows other points of interest. The steep mixing line found by CG between North Atlantic Deep Water (NADW; salinity  $\sim 34.95$  psu,  $\delta^{18}\text{O} \sim 0.0\text{‰}$ ) and Antarctic Bottom Water (AABW; salinity  $\sim 34.65$  psu,  $\delta^{18}\text{O} \sim -0.6\text{‰}$ ) is now clear. However, separation of the data from waters deeper than 2500 m in the Atlantic (Figure 4a) and Pacific (Figure 4b) reveals a different relationship in each basin. In the Atlantic (Figure 4a) the deep water mixing line is two-pronged, due to the combined contributions of AABW and Antarctic Intermediate Water (AAIW; salinity  $\sim 34.2$  psu,  $\delta^{18}\text{O} \sim -0.3\text{‰}$ ): the classical extratropical mixing line of CG (Figure 3a) is thus a result of direct mixing of only AAIW and NADW. In the Pacific the deep waters are much better mixed with respect to salt than in the Atlantic [Reid, 1997]. In Figure 4a the mixing line is essentially along the 34.7 isohaline, with the southwest Pacific tending to be 0.03–0.04 psu saltier than the rest of the basin (saltier squares in Figure 4b). However, Figure 4b does show two features in the north (asterisk) and southeastern (fresher squares) Pacific. One is a detectable difference in the contribution of AABW to water characteristics (visible in the amount of  $^{18}\text{O}$  depletion between 0.0 and  $-0.25\text{‰}$ ). The other is a distinct combination of AAIW and NADW (near 34.65 psu) that is  $\sim 0.05$  psu fresher than the endmember of this mixing for the deep waters of the Atlantic (see Figure 4a). Henceforth this combination will be called Circumpolar Deep Water (CPDW). The  $\delta^{18}\text{O}$  may therefore be a useful tracer for the deepwater circulation of the Pacific, although it is worth noting the high

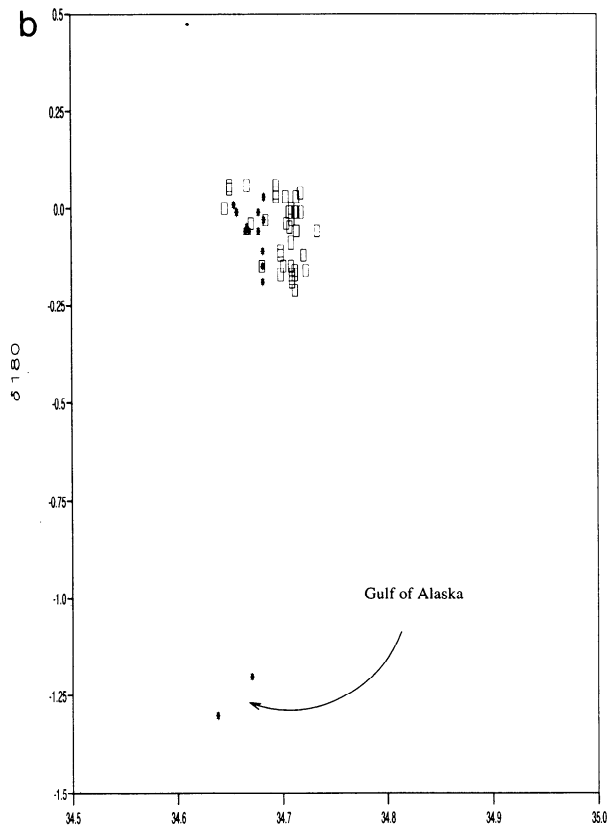
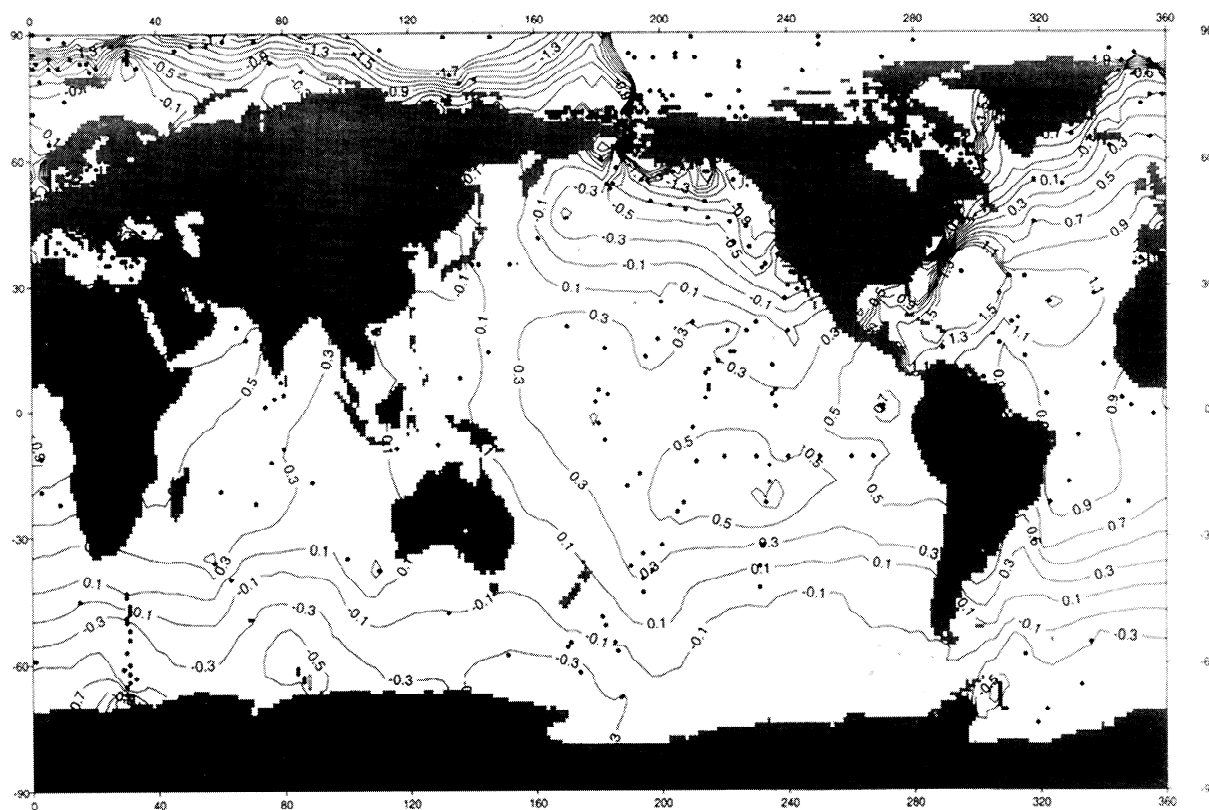


Figure 4. Scatterplot of data points from deeper than 2500 m with a salinity  $S \in [34.5, 35.5]$ : (a) Atlantic Ocean and (b) Pacific Ocean. For code to regional symbols see Figure 3. Note the outliers with very depleted  $\delta^{18}\text{O}$  from the Gulf of Alaska in Figure 4b.



**Figure 5.** Contour diagram of surface  $\delta^{18}\text{O}$  distribution. The very  $^{18}\text{O}$ -depleted river outflows are not shown for clarity; similarly contouring ceases below  $-2\text{‰}$  because of the sharp gradients in the Canadian Arctic and above  $1.5\text{‰}$  because of the figure's resolution of the Mediterranean. Note the maxima in western boundary currents, where  $^{18}\text{O}$ -enriched subtropical water is advected poleward, and the minima in the Californian Coastal Current stemming from the Gulf of Alaska. Data points on which the contouring is based are shown as an asterisk. There are too few in the western Pacific to resolve the Kuroshio.

precision that must be achieved in measurement to extract a signal here. Currently, however, there are only a handful of data points that could be used for this purpose.

### 3. North Pacific

#### 3.1. Shallow Convection in the North Central Pacific

The full data set (Figure 3a) also shows a mixing line not seen by CG, *Ferronksy and Brezgunov* [1982], or *Schmidt* [1998]. This is between fresh,  $\delta^{18}\text{O}$ -enriched water (North Pacific Upper Water (NPUW) - salinity  $< 32.5\text{‰}$ ,  $\delta^{18}\text{O} \sim 0.9\text{‰}$ ) and a region of the main mixing line (salinity  $\sim 34.2\text{‰}$ ,  $\delta^{18}\text{O} \sim -0.3\text{‰}$ ). This freshness indicates mixing that originates within the upper thermocline (shallower than 100 m; compare with the much deeper CPDW discussed above) and north of the Kuroshio extension. Note also that the NPUW cannot have come from the main convection region of the northern Pacific, the Sea of Okhotsk. This is because the latter's outflow extends too deeply (typically to  $\sigma_\theta \sim 27.0\text{ kg m}^{-3}$  [*Freeland et al.*, 1998] or sometimes as deep as  $27.4\text{ kg m}^{-3}$  [*Talley*, 1991]) and the seawater is depleted, rather than enriched, in  $\delta^{18}\text{O}$  throughout this region (G. Winkler, personal communication, 1999).

While the northwest Pacific is very data scarce (Figure 1), this NPUW appears to originate from shallow winter convection at, and north of, the boundary of the Kuroshio extension in the North central Pacific and the subpolar gyre. This is in the region of the

outcropping of the  $\sigma_\theta = 26.0\text{ kg m}^{-3}$  isopycnal [*Reid*, 1997]. Note also the consistency with the clear recent atmospheric exposure of the water around 100 m shown by CFC measurements along  $47^\circ\text{N}$  [*Warner et al.*, 1996]. Normally, subpolar waters have low surface  $\delta^{18}\text{O}$  because of very isotopically depleted precipitation [*Dansgaard*, 1964]. However, western boundary current advection of subtropical waters, which have high  $\delta^{18}\text{O}$  because of the excess evaporation in their source region, alters this surface tendency, as is best illustrated in the Atlantic because data are very scarce in the western Pacific (Figure 5). Only in the approaches to the Bering Sea is there sufficient data to show some evidence for this interpretation. *Tomczak and Godfrey* [1996] show a northward moving arm of the subpolar gyre at around  $170^\circ\text{W}$  that could transport some of this  $\delta^{18}\text{O}$ -enriched water. In Figure 6 we show a typical upper ocean vertical profile from near the Amchitka Pass, through which a strong current advects Pacific water into the Bering Sea [*Reed*, 1990; *Overland et al.*, 1994]. Unlike most of the region (see Figure 5) there is  $\delta^{18}\text{O}$ -enriched water in this area that can only have come from the south. More observations of  $\delta^{18}\text{O}$  in the northwest Pacific are required to confirm this hypothesis.

#### 3.2. Gulf of Alaska

A distinct anomaly is apparent in most of the figures containing data from the Pacific but it is particularly well illustrated by Figure 4b, giving the deep Pacific data. Two data

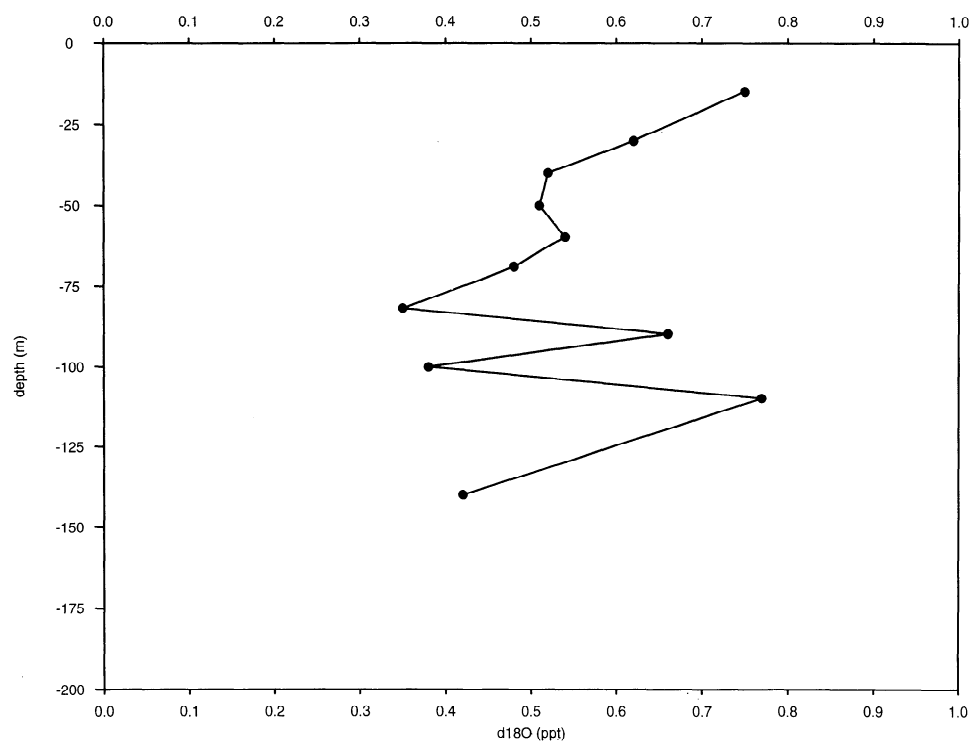


**Figure 6.** Vertical profile of  $\delta^{18}\text{O}$  data from *Cooper et al.*, [1997] at  $\sim(54.4^\circ\text{N}, 165.2^\circ\text{W})$  (data points shown as solid circles).

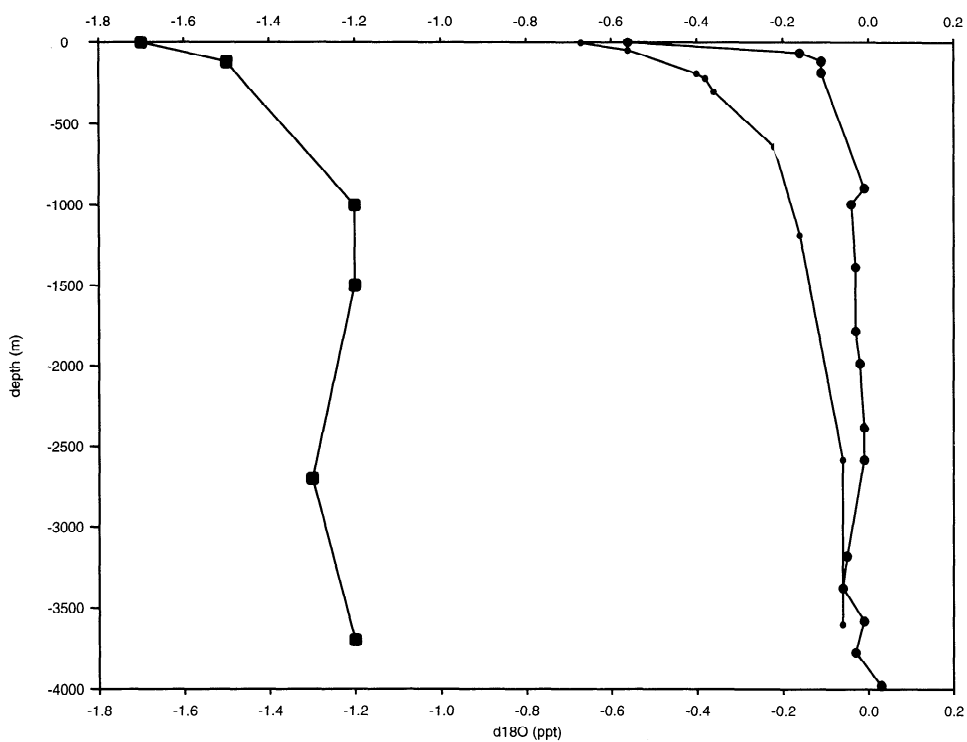


**Figure 7.** Vertical profile of  $\delta^{18}\text{O}$  data from *Kipphut* [1990] at  $\sim(57^\circ\text{N}, 147^\circ\text{W})$  (data points shown as solid squares), contrasting with a typical southern Bering Sea [*Cooper et al.*, 1997] profile from near the Aleutians at  $(53^\circ\text{N}, 177^\circ\text{W})$  (data points shown as small dots) and a subtropical North Pacific profile [*Östlund et al.*, 1987b] at  $(23^\circ\text{N}, 122^\circ\text{W})$  (data points shown as large solid circles).

points have the same salinity as the rest of the basin, but extremely depleted  $\delta^{18}\text{O}$  values of  $\sim -1.2$  ‰. These, plus shallower, points are also clearly seen as isolated points in Figure 3b. A number of even shallower points from the North Pacific with similar oxygen isotope values, but lower salinities, are seen in Figure 3a. These data points originate from the Gulf of Alaska, from observations taken in the late summer of 1982 and 1983 [Kipphut, 1990] and have been verified by the original author.

A vertical profile of these points is shown in Figure 7, along with a typical profile from the Bering Sea just north of the Aleutians [Cooper *et al.*, 1997] and a subtropical North Pacific profile [Östlund *et al.*, 1987b]. While the upper ocean data from Kipphut [1990] are not dissimilar from coastal values around Alaska (Figure 5), the data are clearly much more depleted than would be expected from samples collected in the rest of the deep North Pacific (Figure 4b). There may be an artificial offset of about -1‰ throughout these Gulf of Alaska data. The only possible nearby convection site [Warner and Roden, 1995] with depleted surface waters is in the Bering Sea, where the  $\delta^{18}\text{O}$ -depleted surface waters are restricted to the Alaskan shelf (Figure 5). There is, however, no evidence in the extensive data set from the main Bering Sea (see Figure 1) for very  $\delta^{18}\text{O}$ -depleted water at any subthermocline level above the deepest sill connecting the sea to the North Pacific through the Kamchatka Strait. Local deep convection is theoretically very improbable [Warren, 1983]. There is no clear spreading of the isotopically depleted water beyond the Gulf of Alaska. While there is strong interannual modulation of intermediate level convection in the Northeast Pacific, the deepest reported depth of this is to a  $\sigma_\theta$  of 27.2 kg m<sup>-3</sup> in 1984-1985 [Van Scoy *et al.*, 1991]. Resolution of the reality of this anomaly awaits a future observational programme in the very poorly sampled northeast Pacific.

#### 4. Conclusions

We have gathered together a large database of published oxygen isotopic data and have illustrated some uses of this tracer that complement more traditional tracers such as salinity or oxygen. The geographical and temporal coverage of the database is still far from adequate for a true global description of  $\delta^{18}\text{O}$ . However, some of the areas needing additional coverage can be readily identified from our discussion and include much of the northern Pacific, the surface Atlantic, and the Southern Ocean. We make a plea here to the international community to contribute unpublished data to the archive for the use of all. A web site where published data or unpublished data released by agreement with investigators, is in the process of being set up in collaboration with Gavin Schmidt of the NASA Goddard Institute for Space Studies. It will be accessible from <http://www.uea.ac.uk/~e930/oxy18.html>.

Oxygen isotopes, in conjunction with salinity data, have traditionally been very good tracers for the intermixing of ocean waters with runoff, sea ice melting, and brine release caused by sea ice formation. However, we have shown that more recent use of this conservative variable to track water masses also reveals new information about even large-scale mixing processes. The  $\delta^{18}\text{O}$  highlights a distinct difference between the contributions of AAIW and NADW to producing the intermediate and deep waters in the Atlantic and Pacific. It also shows widespread influence in the North Pacific of thermocline water originating from the subpolar gyre boundary in a way not appreciated in previous isotopic studies.

**Acknowledgments.** This study has been financially supported by grant F204Q from the Leverhulme Trust. We gratefully acknowledge the provision of large amounts of Atlantic data to the database by my colleagues Karen Heywood and Michael Meredith, and the observational effort put into that material by their coworkers Russell Frew and Paul Dennis. In addition, Lee Cooper, of the Oak Ridge National Laboratory, kindly provided access to the large collection of Bering Sea and Arctic data. George Kipphut checked the values given by Kipphut [1990]. Gavin Schmidt helped resolve some variation in the sources of GEOSECS isotopic data and forwarded some additional river runoff data. Finally, Martin Wadley helped with interpretations of the Levitus climatology, and the reviewers helped us tighten up some of our interpretations.

#### References

- Andrie, C., and L. Merlivat, Contribution of deuterium,  $\text{O}^{18}$ ,  $\text{He}^3$  and tritium isotopic data to the study of the Red Sea circulation, *Oceanol. Acta*, **12**, 165-174, 1989.
- Archambeau, A. S., C. Pierre, A. Poisson, and B. Schauer, Distribution of oxygen and carbon stable isotopes and CFC-12 in the water masses of the Southern Ocean at 30°E from South Africa to Antarctica: results of the CIVA1 cruise, *J. Mar. Syst.*, **17**, 25-38, 1998.
- Azetsu-Scott, K., and F. C. Tan, Oxygen isotope studies from Iceland to an East Greenland fjord: Behaviour of glacial meltwater plume, *Mar. Chem.*, **56**, 239-251, 1997.
- Baertschi, P., Absolute  $^{18}\text{O}$  of standard mean ocean waters, *Earth Planet. Sci.*, **31**, 341-344, 1976.
- Bauch, D., P. Schlosser, and R. G. Fairbanks, Freshwater balance and the sources of deep and bottom waters in the Arctic Ocean inferred from the distribution of  $\text{H}_2^{18}\text{O}$ , *Prog. Oceanogr.*, **35**, 53-80, 1995.
- Bedard, P., C. Hillairemarcel, and P. Page, O-18 modeling of fresh-water inputs in Baffin Bay and Canadian Arctic coastal waters, *Nature*, **293**, 287-289, 1981.
- Cooper, L. W., T. E. Whitledge, J. M. Grebmeier, and T. Weingartner, The nutrient, salinity, and stable isotope composition of Bering and Chukchi Seas waters in and near the Bering Strait, *J. Geophys. Res.*, **102**, 12,563-12,573, 1997.
- Craig, H., and L. I. Gordon, Isotopic oceanography: Deuterium and oxygen 18 variations in the ocean and the marine atmosphere, in *Stable Isotopes in Oceanographic Studies and Paleotemperatures*, edited by E. Tongiorgi, pp. 9-130, Cons. Naz. di Rech., Spoleto, Italy, 1965.
- Dansgaard, W., Stable isotopes in precipitation, *Tellus*, **16**, 436-468, 1964.
- Duplessy, J. C., A. W. H. Bé, and P. L. Blanc, Oxygen and carbon isotopic composition and biogeographic distribution of planktonic foraminifera in the Indian Ocean, *Palaeogeogr. Palaeoclimatol. Palaeoecol.*, **33**, 9-46, 1981.
- Epstein, S., and T. Mayeda, Variation of  $\delta^{18}\text{O}$  content of waters from natural sources, *Geochim. Cosmochim. Acta*, **4**, 213-224, 1953.
- Fairbanks, R. G., The origin of continental shelf and slope water in the New York Bight and Gulf of Maine: Evidence from  $\text{H}_2^{18}\text{O}/\text{H}_2^{16}\text{O}$  ratio measurements, *J. Geophys. Res.*, **87**, 5796-5808, 1982.
- Ferronsky, V. I., and V. S. Brezgunov, Stable isotopes and ocean dynamics, in *Environmental Isotopes in the Hydrosphere*, edited by V. I. Ferronsky and V. A. Polyakov, pp. 1-27, John Wiley, New York, 1982.
- Freeland, H. J., A. S. Bychkov, F. Whitney, C. Taylor, C. S. Wong, and G. I. Yurasev, WOCE Section P1W in the Sea of Okhotsk. 1, Oceanographic description, *J. Geophys. Res.*, **103**, 15,613-15,623, 1998.
- Frew, R. D., K. J. Heywood, and P. F. Dennis, Oxygen isotope study of water masses in the Princess Elizabeth Trough, Antarctica, *Mar. Chem.*, **49**, 141-153, 1995.
- Frew, R. D., P. F. Dennis, K. J. Heywood, M. P. Meredith, and S. M. Boswell, The oxygen isotope composition of water masses in the northern North Atlantic, *Deep Sea Res.*, in press, 2000.
- Frohlich, K., J. Grabczak, and K. Rozanski, Deuterium and O-18 in the Baltic Sea, *Chem. Geol.*, **72**, 77-83, 1988.
- Gat, J. R., A. Shemesh, E. Tziperman, A. Hecht, D. Georgopoulos, and O. Basturk, The stable isotope composition of waters of the eastern Mediterranean Sea, *J. Geophys. Res.*, **101**, 6441-6451, 1996.
- Grebmeier, J. B., L. W. Cooper, and M. J. DeNiro, Oxygen isotopic composition of bottom seawater and tunicate cellulose used as indicators of water masses in the northern Bering and Chukchi Seas, *Limnol. Oceanogr.*, **35**, 1182-1195, 1990.



- Grossman, E. L., Stable isotope fractionation in live benthic foraminifera from the southern California borderland, *Palaeogeogr. Palaeoclimatol. Palaeoecol.*, **47**, 301-327, 1984.
- Heywood, K. J., R. A. Locarnini, R. D. Frew, P. F. Dennis, and B. A. King, Transport and water masses of the Antarctic slope front system in the eastern Weddell Sea, in *Ocean, Ice, and Atmosphere: Interactions at the Antarctic Continental Margin*, *Antarctic Res. Ser.*, vol. 75, edited by S. S. Jacobs and R. F. Weiss, pp. 203-214, AGU, Washington, D. C., 1998.
- Hoffmann, G., and M. Heimann, Water tracers in the ECHAM GCM, in *Isotope Techniques in the Study of the Past and Current Environmental Changes in the Hydrosphere and the Atmosphere*, Int. At. Energy Agency, Geneva, 1993.
- Hoffmann, G., and M. Heimann, Water isotope modelling in the Asian Monsoon region, *Q. J. Int.*, **37**, 115-128, 1997.
- Joussaume, S., and J. Jouzel, Paleoclimate tracers: An investigation using an atmospheric general circulation model under ice age conditions, *J. Geophys. Res.*, **98**, 2807-2830, 1993.
- Joussaume, S., R. Sadourny, and J. Jouzel, A general circulation model of water isotope cycles in the atmosphere, *Nature*, **311**, 24-29, 1984.
- Jouzel, J., G. L. Russell, R. J. Suzzo, R. D. Koster, J. W. C. White, and W. S. Broecker, Simulations of HDO and H<sub>2</sub><sup>18</sup>O atmospheric cycles using the NASA GISS general circulation model: The seasonal cycle for present-day conditions, *J. Geophys. Res.*, **92**, 14,739-14,760, 1987.
- Khim, B. K., and D. E. Krantz, Oxygen isotopic identity of the Delaware Coastal Current, *J. Geophys. Res.*, **101**, 16,509-16,514, 1996.
- Kipphut, G. W., Glacial meltwater input to the Alaska Coastal Current: Evidence from oxygen isotope measurements, *J. Geophys. Res.*, **95**, 5177-5181, 1990.
- Létole, R., J. M. Martin, A. J. Thomas, V. V. Gordeev, S. Gusarova, and I. S. Sidorov, <sup>18</sup>O abundance and dissolved silicate in the Lena delta and Laptev Sea (Russia), *Mar. Chem.*, **43**, 47-64, 1993.
- Levitus, S., R. Burgett, and T. P. Boyer, *World ocean atlas 1994*, vol. 3, *salinity*, NOAA Atlas NESDIS, **3**, 111 pp., Natl. Oceanic and Atmos. Admin., Silver Spring, Md., 1994.
- MacDonald, R. W., D. W. Paton, E. C. Carmack, and A. Omstedt, The freshwater budget and under-ice spreading of Mackenzie River water in the Canadian Beaufort Sea based on salinity and <sup>18</sup>O/<sup>16</sup>O measurements in water and ice, *J. Geophys. Res.*, **100**, 895-919, 1995.
- Meredith, M. P., K. E. Grose, E. L. McDonagh, K. J. Heywood, R. D. Frew, and P. Dennis, The distribution of oxygen isotopes in the water masses of Drake Passage and the South Atlantic, *J. Geophys. Res.*, **104**, 20,949-20,962, 1999a.
- Meredith, M. P., K. J. Heywood, R. D. Frew, and P. Dennis, Formation and circulation of the water masses between the southern Indian Ocean and Antarctica: Results from <sup>δ</sup><sup>18</sup>O, *J. Mar. Res.*, **57**, 449-470, 1999b.
- Merlivat, L., F. Pineau, and M. Javoy, Hydrothermal vent waters at 13°N on the East Pacific Rise: Isotopic composition and gas concentration, *Earth Planet. Sci. Lett.*, **84**, 100-108, 1987.
- Mook, W. G., The oxygen-18 content of rivers, *SCOPE*, **52**, 565-570, 1982.
- Moore, R. M., M. G. Lowings, and F. C. Tan, Geochemical profiles in the central Arctic Ocean: Their relation to freezing and shallow circulation, *J. Geophys. Res.*, **88**, 2667-2674, 1983.
- Östlund, H. G., and G. Hut, Arctic Ocean water mass balance from isotope data, *J. Geophys. Res.*, **89**, 6373-6381, 1984.
- Östlund, H. G., G. Possner, and J. H. Swift, Ventilation rate of the deep Arctic Ocean from carbon-14 data, *J. Geophys. Res.*, **92**, 3769-3777, 1987a.
- Östlund, H. G., H. Craig, W. S. Broecker, and D. Spenser, GEOSECS Atlantic, Pacific and Indian Ocean expeditions: Shorebased data and graphics, vol. 7, *technical report*, 200 pp., Nat. Sci. Found., Washington, D. C., 1987b.
- Overland, J. E., M. C. Spillane, H. E. Hurlburt, and A. J. Wallcraft, A numerical study of the circulation of the Bering Sea Basin and exchange with the North Pacific Ocean, *J. Phys. Oceanogr.*, **24**, 736-758, 1994.
- Pickard, G. L., and W. J. Emery, *Descriptive Physical Oceanography*, 4th ed., 249 pp., Pergamon, Tarrytown, N.Y., 1982.
- Pierre, C., The oxygen and carbon isotope distribution in the Mediterranean water masses, *Mar. Geol.*, **153**, 41-55, 1999.
- Pierre, C., C. Vergnaud-Grazzini, and J. C. Faugeres, Oxygen and carbon stable isotope tracers of the water masses of the central Brazil Basin, *Deep Sea Res.*, **38**, 597-606, 1991.
- Pierre, C., A. Vangriesheim, and E. Laube-Lenfant, Variability of water masses and of organic production-regeneration systems as related to eutrophic, mesotrophic and oligotrophic conditions in the northeast Atlantic Ocean, *J. Mar. Syst.*, **5**, 159-170, 1994.
- Reed, R. K., A year-long observation of water exchange between the North Pacific and the Bering Sea, *Limnol. Oceanogr.*, **35**, 1604-1609, 1990.
- Reid, J. L., On the total geostrophic circulation of the Pacific Ocean: flow patterns, tracers, and transports, *Prog. Oceanogr.*, **39**, 263-352, 1997.
- Rohling, E. J., and G. R. Bigg, Paleosalinity and <sup>δ</sup><sup>18</sup>O: A critical assessment, *J. Geophys. Res.*, **103**, 1307-1318, 1998.
- Schmidt, G. A., Oxygen-18 variations in a global ocean model, *Geophys. Res. Lett.*, **25**, 1201-1204, 1998.
- Stenni, B., P. Nichetto, D. Bregant, P. Scarazzato, and A. Longinelli, The <sup>δ</sup><sup>18</sup>O signal of the northward flow of Mediterranean waters in the Adriatic Sea, *Oceanol. Acta*, **18**, 319-328, 1995.
- Strain, P. M., and F. C. Tan, Seasonal evolution of oxygen isotope-salinity relationships in high-latitude waters, *J. Geophys. Res.*, **98**, 14,589-14,598, 1993.
- Swart, P. K., The oxygen and hydrogen isotopic composition of the Black Sea, *Deep Sea Res.*, **38**, suppl. 2, S761-S772, 1991.
- Talley, L. D., An Okhotsk sea-water anomaly: Implications for ventilation in the North Pacific, *Deep Sea Res.*, **38S**, S171-S190, 1991.
- Tan, F. C., and P. M. Strain, The distribution of sea-ice meltwater in the eastern Canadian Arctic, *J. Geophys. Res.*, **85**, 1925-1932, 1980.
- Tan, F. C., and P. M. Strain, Sea-ice and oxygen isotopes in Foxe Basin, Hudson Bay, and Hudson Strait, Canada, *J. Geophys. Res.*, **101**, 20,869-20,876, 1996.
- Tomczak, M., and J. S. Godfrey, *Regional Oceanography: An Introduction*, 422 pp., Pergamon, Tarrytown, N.Y., 1996.
- Van Donk, J., and G. Mathieu, Oxygen isotope compositions of foraminifera and water samples from the Arctic Ocean, *J. Geophys. Res.*, **74**, 3396-3408, 1969.
- Van Scoy, K. A., D. B. Olson, and R. A. Fine, Ventilation of North Pacific Intermediate Waters: The role of the Alaskan Gyre, *J. Geophys. Res.*, **96**, 16,801-16,810, 1991.
- Vetshteyn, V. Y., G. A. Malyuk, and V. P. Rusanov, Oxygen-18 distribution in the central Arctic Basin, *Oceanology*, **14**, 514-519, 1976.
- Warner, M. J., and G. I. Roden, Chlorofluorocarbon evidence for recent ventilation of the deep Bering Sea, *Nature*, **373**, 409-412, 1995.
- Warner, M. J., J. L. Bullister, D. P. Wisegarver, R. H. Gammon, and R. F. Weiss, Basin-wide distributions of chlorofluorocarbons CFC-11 and CFC-12 in the North Pacific: 1985-1989, *J. Geophys. Res.*, **101**, 20,525-20,542, 1996.
- Warren, B. A., Why is no deep water formed in the North Pacific?, *J. Mar. Res.*, **41**, 327-347, 1983.
- Weiss, R. F., H. G. Östlund, and H. Craig, Geochemical studies of the Weddell Sea, *Deep Sea Res.*, **26**, 1093-1120, 1979.
- Wellington, G. M., R. B. Dunbar, and G. Merlen, Calibration of stable oxygen isotope signatures in Galapagos corals, *Paleoceanography*, **11**, 467-480, 1996.
- Weppernig, R., P. Schlosser, S. Khatiwala, and R. G. Fairbanks, Isotope data from Ice Station Weddell: Implications for deep water formation in the Weddell Sea, *J. Geophys. Res.*, **101**, 25,723-25,739, 1996.

G. R. Bigg School of Environmental Sciences,  
University of East Anglia, Norwich NR4 7TJ, England. (e-mail: g.bigg@uea.ac.uk)

E. J. Rohling, School of Ocean and Earth Sciences, University of Southampton, Southampton Oceanography Centre, Southampton SO14 3ZH, England.

(Received November 18, 1998; revised September 21, 1999;  
accepted November 10, 1999.)